

Induced superconducting pairing in integer quantum Hall edge states

Mehdi Hatefipour¹, Joseph J. Cuzzo², Jesse Kanter¹, William M. Strickland¹,
Christopher R. Allemang³, Tzu-Ming Lu^{3,4}, Enrico Rossi², and Javad Shabani^{1*}

¹Center for Quantum Phenomena, Department of Physics, New York University, NY 10003, USA

²Department of Physics, William & Mary, Williamsburg, Virginia 23187, USA

³Sandia National Laboratories, Albuquerque, New Mexico 87185, USA

⁴Center for Integrated Nanotechnologies, Sandia National Laboratories, Albuquerque, New Mexico, 87123, USA

(Dated: April 7, 2022)

Indium Arsenide (InAs) near surface quantum wells (QWs) are promising for the fabrication of semiconductor-superconductor heterostructures given that they allow for a strong hybridization between the two-dimensional states in the quantum well and the ones in the superconductor. In this work we present results for InAs QWs in the quantum Hall regime placed in proximity of superconducting NbTiN. We observe a negative downstream resistance with a corresponding reduction of Hall (upstream) resistance, consistent with a very high Andreev conversion. We analyze the experimental data using the Landauer-Büttiker formalism, generalized to allow for Andreev reflection processes. We attribute the high efficiency of Andreev conversion in our devices to the large transparency of the InAs/NbTiN interface and the consequent strong hybridization of the QH edge modes with the states in the superconductor.

Anyons with non-Abelian statistics are of great fundamental interest [1] and can be used to realize topologically protected, and therefore intrinsically fault-tolerant qubits [2–4]. Non-Abelian anyons are expected to be realized in few fractional quantum Hall (QH) states [5–9] such as the QH states with filling factor $\nu = \frac{5}{2}$ [10–12], and, possibly, $\nu = \frac{12}{5}$ [13]. However, so far, no unambiguous experimental confirmation exists of the presence of non-Abelian anyons in such QH states.

An alternative route to realize non-Abelian anyons relies on inducing superconducting pairing between counter-propagating edge modes of QH states that, intrinsically, support only Abelian anyons [14–17]. These theoretical proposals build on an earlier proposal for creating Majorana zero modes, the anyons with the simplest non-Abelian statistics, using 1D modes at the edge of a 2D topological insulator (TI) in contact with a superconductor (SC) [18]. In contrast to TIs, in two-dimensional electron gases (2DEGs) in the QH regime, by varying filling factor ν , states can be realized with a variety of topological orders. This allows access to more exotic edge states needed for engineering anyons with richer non-Abelian statistics. Key in all these theoretical proposals is the ability to induce superconducting pairing, via the proximity effect, between the QH edge modes.

The strength of the superconducting correlations that can be induced in a QH-SC heterojunction can be evaluated by obtaining the amplitude of the Andreev reflection of QH edge modes. The early search for Andreev reflection in QH-SC systems focused on InAs and InGaAs semiconductor magneto-resistance oscillations at relatively low magnetic fields [19] fol-

lowed later by reports of induced superconductivity in QH states [20]. More recently there have been reports of observation of induced superconductivity [21, 22], cross Andreev conversion [23, 24], edge state mediated supercurrent [25], and interference of chiral Andreev edge states [26–29] in graphene. To make further progress, it is essential to reliably demonstrate the ability to induce robust superconducting correlations into the edge modes of a QH state.

In this work we show that in high quality InAs/NbTiN heterostructures, very strong superconducting correlations can be induced in the edge modes of integer QH states realized in the InAs-based quantum wells (QWs). Such correlations appear to be robust, showing no oscillations as a function of doping, for gate voltages within the QH plateaus. We analyze the experimental data in conjunction with a microscopic model to extract the details of the processes determining the transport properties of the QH-SC interface.

Figure 1(a) shows a cross sectional schematic of the fabricated device used in this work. The QW is formed by a 4 nm layer of $\text{In}_{0.81}\text{Ga}_{0.19}\text{As}$ layer, a 7 nm layer of InAs, and a 10 nm top layer of $\text{In}_{0.81}\text{Ga}_{0.19}\text{As}$. The QW is grown on $\text{In}_x\text{Al}_{1-x}\text{As}$ buffer where the indium content is step-graded from $x = 0.52$ to 0.81. A delta-doped Si layer with electron doping $n \sim 1 \times 10^{12} \text{ cm}^{-2}$ is placed 6 nm below the QW. This epitaxial structure has been used in previous studies on mesoscopic superconductivity [30–33], in the development of tunable qubits [34], and in studies aimed at realizing and detecting topological superconducting states [35–37].

A Hall bar, Fig. 1(b), is fabricated by electron

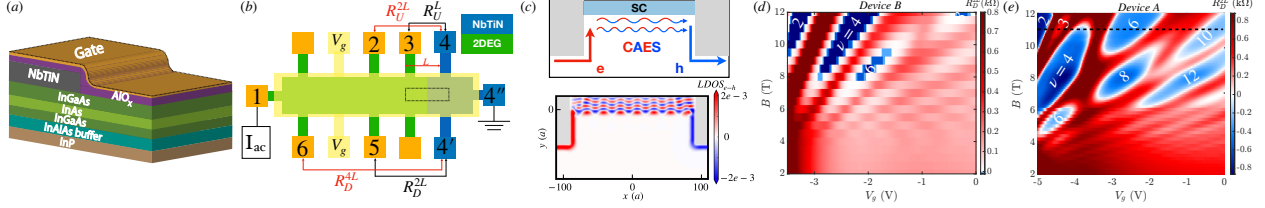


FIG. 1: (a) Schematic of gated NbTiN/InAs hybrid device structure (only the portion which is defined by the rectangle in Fig. 1(b)). (b) Device pin-out configuration. Contacts 1,2,3,5, and 6 are normal; contacts 4, 4', 4'' are superconducting. Contacts 1 and 4'' are used as the source and drain, respectively. Contacts which are not labeled had electrical connection issue during the experiment. (c) Andreev conversion via CAES interference along the QH-SC interface (top) and a supporting tight binding calculation of the difference between the electron and hole LDOS ($LDOS_{e-h}$) (bottom). (d) Measured R_D^{2L} as a function of V_g and B in a dirty interface device (device B). (e) Measured R_D^{2L} as a function of V_g and B in the cleaned interface device (device A). IQHSs are labeled from complementary R_{xy} data. The dashed line shows the position of the cut shown in Fig. 2 (a).

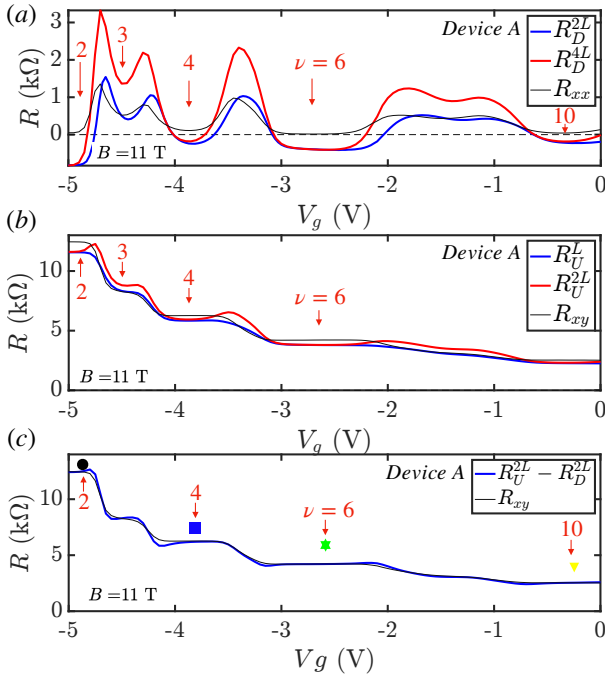


FIG. 2: $R_U - R_D$ and R_{xy} shown as a function of V_g . All traces taken at $B = 11$ T (Device A). IQHSs are labeled and markers are shown for the states used in Fig. 3(c).

beam lithography. In order to study the 2DEG/SC interface, a 90 nm thick layer of NbTiN was sputtered as the superconducting contacts with a $150\mu\text{m}$ -wide interface after performing wet etch surface cleaning (Device A). We also fabricated a similar device with intentional no surface cleaning step before NbTiN sputtering (Device B). A metallic top gate is created by depositing a layer of Al oxide followed by an Al layer to control the QW electron density [38]. The mobility of the QW is determined to be $\mu \sim$

$12,000\text{ cm}^2/\text{V}\cdot\text{s}$ at $n \sim 8.51 \times 10^{11}\text{ cm}^{-2}$ corresponding to an electron mean free path of $l_e \sim 180\text{ nm}$. All data reported here were taken at $T \sim 30\text{ mK}$. We have provided more information on transport properties of the sample in the SI. We note that while we focus mainly on one device (Device A) in the main text, we have studied a few other similar devices which their data have been shown in SI.

When the sample is placed in a magnetic field, in the classical picture, electrons and holes will alternate their skipping orbits across the interface of the superconductor and 2DEG [39]. In the full quantum-mechanical analysis the electron and hole edge states hybridize due to the proximity of the SC and form a coherent chiral Andreev edge state (CAES) extended along the QH-SC interface [27, 40, 41]. A schematic of CAES propagation along the QH-SC interface is shown in Fig. 1 (c). In this picture, if more holes than electrons reach the normal lead downstream from the superconducting electrode (lead 5), then a negative potential difference ($V_5 - V_4'$) develops. In Fig. 1 (c) we also show the the local density of states of a CAES obtained with a tight binding (TB) calculation performed using the python package Kwant [42]. In the TB model the presence of the magnetic field is taken into account via a Peierls phase, and the superconductivity of the QW proximitized by NbTiN via a mean field an s-wave pairing term of strength $\tilde{\Delta}$. The details of the TB model can be found in the SI.

Figures 1(d) and (e) show the results for the downstream resistance, R_D^{2L} , measured between the voltage contacts 5 and 4', as a function of gate voltage V_g and magnetic field B . Hall resistance data measured between contacts 2 and 5 allow us to determine the filling factor of the different regions of Fig. 1 (d), (e). Figure 2(a) shows the horizontal cut at $B = 11\text{ T}$ of Fig. 1(e), R_D^{4L} , and the corresponding

longitudinal resistance R_{xx} . From the R_{xx} measurements we see that we have well developed integer QH states (IQHS). From Figs. 1(e) and 2(a) we clearly observe that R_D is negative for IQHS, a fact that strongly suggests the presence of Andreev processes at the QH-SC interface for these IQHS. We notice the importance of a clean InAs/NbTiN interface by comparing the magnitude of negative resistance in Figs. 1 (d) and (e). The clean interface on device A has been achieved by etching the surface of defined NbTiN pattern area by buffered oxide etchant (BOE) for 2 seconds immediately followed by loading into sputtering tool's load lock in order to minimize the time for the native oxide growth at the interface. On the other hand, for device B and all the other devices mentioned in SI, this cleaning step has been skipped and NbTiN sputtered on the defined region after its exposure to air. For the rest of the paper, we focus only on device A results. The upstream resistance R_U^{2L} (measured between contacts 3 and 4) exhibits plateaus in correspondence to the R_{xy} plateaus in magnetic field but with resistance values lower than R_{xy} . Moreover, $R_U^{2L} - R_D^{2L}$ recovers the quantized Hall value, R_{xy} , as shown in Fig. 2 (c). Note that this difference does not necessarily match the R_{xy} data outside the QH regime.

These results can be understood within the Landauer-Büttiker (LB) theory, generalized to allow for the presence of a superconducting lead [43, 44].

We start with the six-terminal setup shown in Fig. 1(b) (see also the SI). We assume the terminal 1, 2, 3, 5, 6 to be ideal metallic leads, and contact 4 to be a superconducting lead. We first consider the limit in which no normal reflection or transmission processes take place at the superconducting lead. Let I_i , V_i , the currents and voltages, respectively, at the terminals $i = (1, 2, 3, 4, 5, 6)$. Without loss of generality, we can set $V_4 = 0$. We can use the charge conservation equation $\sum_i I_i = 0$ to express I_4 in terms of the currents at the other leads. With these considerations the LB equations reduce to the following system of linear equations:

$$\begin{pmatrix} I_1 \\ I_2 \\ I_3 \\ I_5 \\ I_6 \end{pmatrix} = \frac{\nu}{R_H} \begin{pmatrix} 1 & 0 & 0 & 0 & -1 \\ -1 & 1 & 0 & 0 & 0 \\ 0 & -1 & 1 & 0 & 0 \\ 0 & 0 & 2A - 1 & 1 & 0 \\ 0 & 0 & 0 & -1 & 1 \end{pmatrix} \begin{pmatrix} V_1 \\ V_2 \\ V_3 \\ V_5 \\ V_6 \end{pmatrix} \quad (1)$$

where ν is the number of edge states, R_H is the Hall resistance, and A is the average probability, per edge mode, of Andreev reflection. Considering that no current flows into leads 2, 3, 5, 6, so that $I_2 = I_3 = I_5 = I_6 = 0$, and $V_1 = V_2 = V_3$, $V_5 = V_6$, and

setting $I \equiv I_1$, it is straightforward to solve Eq. (1) to obtain

$$R_U^{2L} = \frac{V_2}{I} = \frac{R_H}{\nu} \frac{1}{2A} \quad (2)$$

$$R_D^{2L} = \frac{V_5}{I} = \frac{R_H}{\nu} \left(\frac{1}{2A} - 1 \right) \quad (3)$$

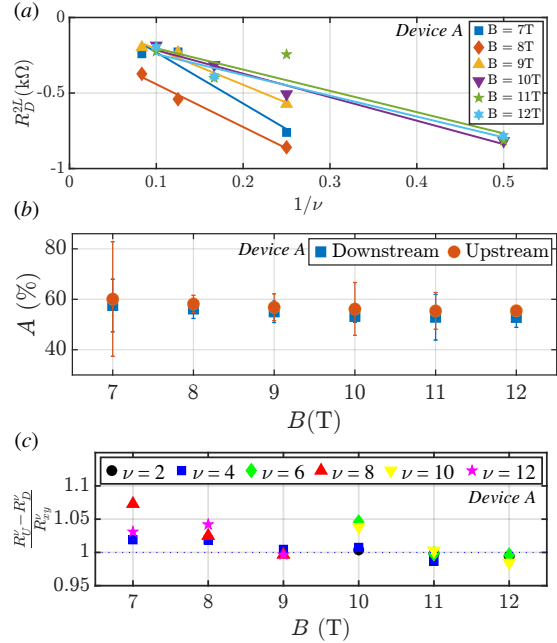


FIG. 3: (a) R_D^{2L} vs $1/\nu$ for different IQHSs and values of B , and linear fits corresponding to each magnetic field. (b) A obtained from the slope of linear fits to R_D and R_U data vs $1/\nu$ with their corresponding error bars. (c) $(R_U^{2L} - R_D^{2L})/R_{xy}$ for different ν s and values of B .

Figure 3 (a) shows the scaling of R_D with respect to $1/\nu$ for different values of B . From the slope of the fits to the experimental data shown in Fig. 3 (a) we obtain the value of $A_{\text{exp}} = 55\%$, independent, to very good approximation, on the value of V_g within the QH plateaus. Figure 3 (c) shows the consistency of the measured values of R_D^{2L} and R_U^{2L} with the LB predictions by plotting the ratio $(R_U^{2L} - R_D^{2L})/R_{xy}$ as function of B that, according to Eqs. (2-3), is expected to be equal to 1.

To understand qualitatively how such values of A can arise, we consider an effective 1D Bogoliubov de Gennes Hamiltonian, H_{BdG} , for the 1D chiral edge modes: $H_{BdG} = \int dx \psi^\dagger(x) \mathcal{H}(x) \psi(x)$ where $\psi(x) = (c_{x\uparrow}, c_{x\downarrow}^\dagger)$ is the spinor formed by the annihilation (creation) operator for a fermion at position x and spin up (down) and $\mathcal{H}(x) = v_d(-i\partial_x)\tau_0 - v_d k_F \tau_z +$

$\tilde{\Delta}\tau_x$. Here, and in the remainder, we set $\hbar = 1$. In the equation for $H(x)$, v_d is the drift velocity of the edge modes, τ_i are the Pauli matrices Nambu space, k_F is the edge modes Fermi wave vector (measured with respect to the QH-SC interface)

and $\tilde{\Delta}$ is the superconducting pairing induced via the proximity effect by the superconducting lead. Using the expression for H we can obtain the transfer matrix M relating $\psi(x)$ at the two ends of the length L_{sc} of the QH-SC interface (see SI) [40, 45], and then the expression for the electron-hole conversion probability

$$A = \frac{\sin^2(\delta\phi)}{[1 + (v_d k_F / \tilde{\Delta})^2]}. \quad (4)$$

In Eq. (4), $\delta\phi$ is the difference of the phases accumulated by the electron-like and hole-like edge modes along the length of the QH-SC interface. Let $k_F^{(e)}$, $k_F^{(h)}$ be the Fermi wave vector of the electron-like and hole-like edge modes, and $\delta k \equiv |k_F^{(e)} - k_F^{(h)}| = [\tilde{\Delta}^2 + (v_d k_F)^2]^{1/2} / v_d$. We then write $\delta\phi = L_{sc} \delta k$.

Considering that $L_{sc} = 150\mu\text{m}$ is quite large any small change of δk , induced for example by changes in V_g , should result in a significant change of A and therefore of R_U and R_D . However, in the experiment, within the QH plateaus, R_U and R_D do not show any oscillation as a function of V_g . It is natural to conclude that this might be due to scattering processes leading to a dephasing of the electron-like and hole-like modes along the QH-SC interface [28]. In this case the effective A_{eff} can be obtained by averaging over L_{sc} on the right hand side of Eq. (4) to obtain $A_{\text{eff}} = \langle A \rangle = (1/2)[1 + (v_d k_F / \tilde{\Delta})^2]$. Considering that $(v_d k_F / \tilde{\Delta})^2 > 0$ we see that in this case we cannot recover the value of A extracted from the experimental results, $A = 0.55 > 0.5$.

To explain the large value of A , accompanied by the lack of oscillations as a function of V_g , we are led to two possibilities. The first possibility is that δk does not change appreciably as a function of V_g . From Eq. (4), considering that $0 < \sin^2(\delta\phi) < 1$, we can see that to have $A = 0.55$ we must have $v_d k_F / \tilde{\Delta} < 0.9$. In the limit when $\delta\phi$ is such that $\sin^2(\delta\phi) \approx 0.55$, we must have $v_d k_F / \tilde{\Delta} \ll 1$. In this limit we can write $\delta k \approx \tilde{\Delta} / v_d$. Considering that to good approximation, $\tilde{\Delta}$ and v_d are independent of V_g , we recover the observed values of R_U and R_D , with no oscillations, in the QH plateaus. Notice that the condition $v_d k_F / \tilde{\Delta} \ll 1$ is equivalent to the condition $\delta k \xi \approx 1$, where $\xi \equiv v_d / \tilde{\Delta}$ can be interpreted as the superconducting coherence length of the edge modes in proximity of the SC. The other possibility is that dephasing processes are

accompanied by a finite probability of single electron tunneling into the superconductor and breaking of particle-hole (p-h) symmetry. This would allow to have a situation in which electron-like states are more likely than h-like states to tunnel into the superconductor and therefore contribute less to the downstream current explaining a negative R_D even when $A \leq 1/2$. If we denote by T the probability, per edge mode, of an electron-like state to tunnel in the SC, in Eqs. (2), (3) we would replace $2A$ with $2A + T$. In this case from the measurements of R_U and R_D we recover $2A + T$. Assuming $\langle A \rangle = 1/2$ would imply $T = 0.2$. The smallest value of $\langle A \rangle$, consistent with particle conservation, is 15% to which it would correspond $T = 0.8$, a value that implies a very strong breaking of particle-hole symmetry at the QH-SC interface. It is difficult to distinguish between these two possibilities given that we cannot measure separately the quasiparticle and supercurrent contributions to the charge current flowing from the QH region into the superconducting lead.

In conclusion, we have fabricated a quantum Hall-superconductor (QH-SC) epitaxial heterostructure based on InAs and NbTiN and characterized the transport properties of its QH edge modes propagating along a superconducting interface. We have observed negative values for the downstream resistance R_D between a normal lead and the superconducting lead and a corresponding suppression of the upstream resistance R_U such that in the QH plateaus the difference $R_U - R_D$ is equal to the Hall resistance R_H . The negative values of R_D are an unambiguous sign that at the QH-SC interface there is a very large electron-hole conversion probability, A . Using a Landauer-Büttiker analysis we were able to explain the relation between R_D and R_U and express both resistances in terms of a single effective probability for Andreev reflections at the QH-SC interface. Our analysis led us to the conclusion that either the edge modes propagate along the QH-SC interface with negligible dephasing resulting in an electron-hole conversion close to 55%, or, if dephasing processes dominate, that a strong breaking of particle-hole symmetry at the QH-SC interface must occur.

Even the lower bounds estimates for A that we extract from our measurements are remarkable, larger than any published results for QH-SC devices. This shows that in our InAs devices very strong superconducting correlations can be induced into the QH edge modes, an essential prerequisite to use QH-SC heterojunctions to realize non-Abelian anyons and topologically protected qubits and quantum gates based on such unusual quantum states.

We thank Dr. Shashank Misra for his insightful comment and feedback. The NYU team acknowledge partial support from DARPA grant no. DP18AP900007 and ONR grant no. N00014-21-1-2450. JJC and ER acknowledge support from ARO Grant No. W911NF-18-1-0290. JJC also acknowledges support from the Graduate Research Fellowship awarded by the Virginia Space Grant Consortium (VSGC). Sandia National Laboratories is a multimission laboratory managed and operated by National Technology and Engineering Solutions of Sandia LLC, a wholly owned subsidiary of Honeywell International Inc. for the U.S. DOE's National Nuclear Security Administration under contract DE-NA0003525. This work was performed, in part, at the Center for Integrated Nanotechnologies, a U.S. DOE, Office of BESs, user facility. This paper describes objective technical results and analysis. Any subjective views or opinions that might be expressed in the paper do not necessarily represent the views of the U.S. DOE or the United States Government.

* Electronic address: jshabani@nyu.edu

- [1] Moore, G.; Read, N. Nonabelions in the fractional quantum hall effect. *Nuclear Physics B* **1991**, *360*, 362–396.
- [2] Kitaev, A. Fault-tolerant quantum computation by anyons. *Annals of Physics* **2003**, *303*, 2–30.
- [3] Das Sarma, S.; Freedman, M.; Nayak, C. Topologically Protected Qubits from a Possible Non-Abelian Fractional Quantum Hall State. *Phys. Rev. Lett.* **2005**, *94*, 166802.
- [4] Nayak, C.; Simon, S. H.; Stern, A.; Freedman, M.; Das Sarma, S. Non-Abelian anyons and topological quantum computation. *Rev. Mod. Phys.* **2008**, *80*, 1083–1159.
- [5] Read, N.; Green, D. Paired states of fermions in two dimensions with breaking of parity and time-reversal symmetries and the fractional quantum Hall effect. *Phys. Rev. B* **2000**, *61*, 10267–10297.
- [6] Cheng, M. Superconducting proximity effect on the edge of fractional topological insulators. *Phys. Rev. B* **2012**, *86*, 195126.
- [7] Alicea, J.; Fendley, P. Topological Phases with Parafermions: Theory and Blueprints. *Annual Review of Condensed Matter Physics* **2016**, *7*, 119–139.
- [8] Vaezi, A. Fractional topological superconductor with fractionalized Majorana fermions. *Phys. Rev. B* **2013**, *87*, 035132.
- [9] Vaezi, A. Superconducting Analogue of the Parafermion Fractional Quantum Hall States. *Phys. Rev. X* **2014**, *4*, 031009.
- [10] Willett, R.; Eisenstein, J. P.; Störmer, H. L.; Tsui, D. C.; Gossard, A. C.; English, J. H. Observation of an even-denominator quantum number in the fractional quantum Hall effect. *Phys. Rev. Lett.* **1987**, *59*, 1776–1779.
- [11] Miller, J. B.; Radu, I. P.; Zumbühl, D. M.; Levenson-Falk, E. M.; Kastner, M. A.; Marcus, C. M.; Pfeiffer, L. N.; West, K. W. Fractional quantum Hall effect in a quantum point contact at filling fraction $5/2$. *Nature Physics* **2007**, *3*, 561–565.
- [12] Radu, I. P.; Miller, J. B.; Marcus, C. M.; Kastner, M. A.; Pfeiffer, L. N.; West, K. W. Quasi-Particle Properties from Tunneling in the $\nu = 5/2$ Fractional Quantum Hall State. *Science* **2008**, *320*, 899–902.
- [13] Zhu, W.; Gong, S. S.; Haldane, F. D. M.; Sheng, D. N. Fractional Quantum Hall States at $\nu = 13/5$ and $12/5$ and Their Non-Abelian Nature. *Phys. Rev. Lett.* **2015**, *115*, 126805.
- [14] Qi, X. L.; Hughes, T. L.; Zhang, S. C. Chiral topological superconductor from the quantum Hall state. *Physical Review B - Condensed Matter and Materials Physics* **2010**,
- [15] Lindner, N. H.; Berg, E.; Refael, G.; Stern, A. Fractionalizing Majorana Fermions: Non-Abelian Statistics on the Edges of Abelian Quantum Hall States. *Phys. Rev. X* **2012**, *2*, 041002.
- [16] Clarke, D. J.; Alicea, J.; Shtengel, K. Exotic circuit elements from zero-modes in hybrid superconductor–quantum-Hall systems. *Nature Physics* **2014**, *10*, 877–882.
- [17] Mong, R. S. K.; Clarke, D. J.; Alicea, J.; Lindner, N. H.; Fendley, P.; Nayak, C.; Oreg, Y.; Stern, A.; Berg, E.; Shtengel, K.; Fisher, M. P. A. Universal Topological Quantum Computation from a Superconductor-Abelian Quantum Hall Heterostructure. *Phys. Rev. X* **2014**, *4*, 011036.
- [18] Fu, L.; Kane, C. L. Superconducting Proximity Effect and Majorana Fermions at the Surface of a Topological Insulator. *Phys. Rev. Lett.* **2008**, *100*, 096407.
- [19] Nitta, J.; Akazaki, T.; Takayanagi, H. Magnetic-field dependence of Andreev reflection in a clean Nb-InAs-Nb junction. *Physical review. B, Condensed matter* **1994**, *49*, 3659–3662.
- [20] Wan, Z.; Kazakov, A.; Manfra, M. J.; Pfeiffer, L. N.; West, K. W.; Rokhinson, L. P. Induced superconductivity in high-mobility two-dimensional electron gas in gallium arsenide heterostructures. *Nature Communications* **2015**, *6*, 7426 EP –.
- [21] Rickhaus, P.; Weiss, M.; Marot, L.; Schönenberger, C. Quantum Hall Effect in Graphene with Superconducting Electrodes. *Nano Letters* **2012**, *12*, 1942.
- [22] Park, G.-H.; Kim, M.; Watanabe, K.; Taniguchi, T.; Lee, H.-J. Propagation of superconducting coherence via chiral quantum-Hall edge channels. *Scientific Reports* **2017**, *7*, 10953.
- [23] Önder Gül; Ronen, Y.; Lee, S. Y.; Shapourian, H.; Zauberman, J.; Lee, Y. H.; Watanabe, K.; Taniguchi, T.; Vishwanath, A.; Yacoby, A.; Kim, P.

- Induced superconductivity in the fractional quantum Hall edge. 2021.
- [24] Lee, G.-H.; Huang, K.-F.; Efetov, D. K.; Wei, D. S.; Hart, S.; Taniguchi, T.; Watanabe, K.; Yacoby, A.; Kim, P. Inducing superconducting correlation in quantum Hall edge states. *Nature Physics* **2017**, *13*, 693–698.
- [25] Amet, F.; Ke, C. T.; Borzenets, I. V.; Wang, J.; Watanabe, K.; Taniguchi, T.; Deacon, R. S.; Yamamoto, M.; Bomze, Y.; Tarucha, S.; Finkelstein, G. Supercurrent in the quantum Hall regime. *Science* **2016**, *352*, 966–969.
- [26] Zhao, L.; Arnault, E. G.; Bondarev, A.; Seredinski, A.; Larson, T. F. Q.; Draelos, A. W.; Li, H.; Watanabe, K.; Taniguchi, T.; Amet, F.; Baranger, H. U.; Finkelstein, G. Interference of chiral Andreev edge states. *Nature Physics* **2020**, *16*, 862–867.
- [27] Hoppe, H.; Zülicke, U.; Schön, G. Andreev Reflection in Strong Magnetic Fields. *Phys. Rev. Lett.* **2000**, *84*, 1804–1807.
- [28] Kurilovich, V. D.; Raines, Z. M.; Glazman, L. I. Disorder in Andreev reflection of a quantum Hall edge. 2022; <https://arxiv.org/abs/2201.00273>.
- [29] Manesco, A. L. R.; Flór, I. M.; Liu, C.-X.; Akhmerov, A. R. Mechanisms of Andreev reflection in quantum Hall graphene. 2021; <https://arxiv.org/abs/2103.06722>.
- [30] Kjaergaard, M.; Nichele, F.; Suominen, H.; Nowak, M.; Wimmer, M.; Akhmerov, A.; Folk, J.; Flensberg, K.; Shabani, J.; Palmstrøm, C.; Marcus, C. Quantized conductance doubling and hard gap in a two-dimensional semiconductor-superconductor heterostructure. *Nature communications* **2016**, *7*, 12841.
- [31] Böttcher, C. G. L.; Nichele, F.; Kjaergaard, M.; Suominen, H. J.; Shabani, J.; Palmstrøm, C. J.; Marcus, C. M. Superconducting, insulating and anomalous metallic regimes in a gated two-dimensional semiconductor-superconductor array. *Nature Physics* **2018**, *14*, 1138–1144.
- [32] Mayer, W.; Yuan, J.; Wickramasinghe, K. S.; Nguyen, T.; Dartiailh, M. C.; Shabani, J. Superconducting proximity effect in epitaxial Al-InAs heterostructures. *Applied Physics Letters* **2019**, *114*, 103104.
- [33] Mayer, W.; Dartiailh, M. C.; Yuan, J.; Wickramasinghe, K. S.; Rossi, E.; Shabani, J. Gate controlled anomalous phase shift in Al/InAs Josephson junctions. *Nature Communications* **2020**, *11*, 212.
- [34] Casparis, L.; Pearson, N. J.; Kringhøj, A.; Larsen, T. W.; Kuemmeth, F.; Nygård, J.; Krogstrup, P.; Petersson, K. D.; Marcus, C. M. Voltage-controlled superconducting quantum bus. *Phys. Rev. B* **2019**, *99*, 085434.
- [35] Suominen, H. J.; Kjaergaard, M.; Hamilton, A. R.; Shabani, J.; Palmstrøm, C. J.; Marcus, C. M.; Nichele, F. Zero-Energy Modes from Coalescing Andreev States in a Two-Dimensional Semiconductor-Superconductor Hybrid Platform. *Phys. Rev. Lett.* **2017**, *119*, 176805.
- [36] Fornieri, A. et al. Evidence of topological superconductivity in planar Josephson junctions. *Nature* **2019**, *569*, 89–92.
- [37] Dartiailh, M. C.; Cuzzo, J. J.; Elfeky, B. H.; Mayer, W.; Yuan, J.; Wickramasinghe, K. S.; Rossi, E.; Shabani, J. Missing Shapiro steps in topologically trivial Josephson junction on InAs quantum well. *Nature Communications* **2021**, *12*, 78.
- [38] Shabani, J.; Kjaergaard, M.; Suominen, H. J.; Kim, Y.; Nichele, F.; Pakrouski, K.; Stankevicius, T.; Lutchyn, R. M.; Krogstrup, P.; Feidenhans'l, R.; Kraemer, S.; Nayak, C.; Troyer, M.; Marcus, C. M.; Palmstrøm, C. J. Two-dimensional epitaxial superconductor-semiconductor heterostructures: A platform for topological superconducting networks. *Phys. Rev. B* **2016**, *93*, 155402.
- [39] Chtchelkatchev, N. M.; Burmistrov, I. S. Conductance oscillations with magnetic field of a two-dimensional electron gas-superconductor junction. *Phys. Rev. B* **2007**, *75*, 214510.
- [40] van Ostaay, J. A. M.; Akhmerov, A. R.; Beenakker, C. W. J. Spin-triplet supercurrent carried by quantum Hall edge states through a Josephson junction. *Phys. Rev. B* **2011**, *83*, 195441.
- [41] Khaymovich, I. M.; Chtchelkatchev, N. M.; Shereshevskii, I. A.; Mel'nikov, A. S. Andreev transport in two-dimensional normal-superconducting systems in strong magnetic fields. *EPL (Europhysics Letters)* **2010**, *91*, 17005.
- [42] Groth, C. W.; Wimmer, M.; Akhmerov, A. R.; Waintal, X. Kwant: a software package for quantum transport. *New Journal of Physics* **2014**, *16*, 063065.
- [43] Datta, S.; Bagwell, P. F.; Anantram, M. P. Scattering Theory of Transport for Mesoscopic Superconductors. *ECE Technical Reports. Paper 107* **1996**,
- [44] Beconcini, M.; Polini, M.; Taddei, F. Nonlocal superconducting correlations in graphene in the quantum Hall regime. *Phys. Rev. B* **2018**, *97*, 201403.
- [45] Gao, H.; Xue, H.; Wang, Q.; Gu, Z.; Liu, T.; Zhu, J.; Zhang, B. Observation of topological edge states induced solely by non-Hermiticity in an acoustic crystal. *Phys. Rev. B* **2020**, *101*, 180303.